Systems/Circuits

Role of the Indirect Pathway of the Basal Ganglia in Perceptual Decision Making

Wei Wei,[1,2] **Jonathan E. Rubin,**[3] **and Xiao-Jing Wang**[1,2,4]

[1]Center for Neural Science, New York University, New York, New York 10003, [2]Department of Neurobiology and Kavli Institute for Neuroscience, Yale University School of Medicine, New Haven, Connecticut 06520, [3]Department of Mathematics and Center for the Neural Basis of Cognition, University of Pittsburgh, Pittsburgh, Pennsylvania 15260, and [4]NYU-ECNU Institute of Brain and Cognitive Science, NYU Shanghai, Shanghai, China 200122

The basal ganglia (BG) play an important role in motor control, reinforcement learning, and perceptual decision making. Modeling and experimental evidence suggest that, in a speed–accuracy tradeoff, the corticostriatal pathway can adaptively adjust a decision threshold (the amount of information needed to make a choice). In this study, we go beyond the focus of previous works on the direct and hyperdirect pathways to examine the contribution of the indirect pathway of the BG system to decision making in a biophysically based spiking network model. We find that the mechanism of adjusting the decision threshold by plasticity of the corticostriatal connections is effective, provided that the indirect pathway counterbalances the direct pathway in their projections to the output nucleus. Furthermore, in our model, changes within basal ganglia connections similar to those that arise in parkinsonism give rise to strong beta oscillations. Specifically, beta oscillations are produced by an abnormal enhancement of the interactions between the subthalamic nucleus (STN) and the external segment of globus pallidus (GPe) in the indirect pathway, with an oscillation frequency that depends on the excitatory cortical input to the STN and the inhibitory input to the GPe from the striatum. In a parkinsonian state characterized by pronounced beta oscillations, the mean reaction time and range of threshold variation (a measure of behavioral flexibility) are significantly reduced compared with the normal state. Our work thus reveals a specific circuit mechanism for impairments of perceptual decision making associated with Parkinson's disease.

Key words: **basal ganglia; decision making; Parkinson's disease; indirect pathway**

Introduction

The basal ganglia (BG), working together with the cortex, are crucial for action selection and decision making (Graybiel, 1995; Mink, 1996; Ding and Gold, 2013). In a decision process, a motor response could be triggered when accumulated information about alternative choices reaches a threshold level. A computational study found that the corticostriatal connection can adjust the threshold over a wide range (Lo and Wang, 2006). The proposal, which has gained empirical support from human imaging experiments (Forstmann et al., 2008), demonstrates that speed–accuracy tradeoff in decision making can be implemented by flexibly adjusting the threshold, and the corticostriatal pathway is modifiable through dopamine-dependent synaptic plasticity (Surmeier et al., 2010). In the proposed mechanism, neural activity in the BG output nucleus, the substantia nigra pars reticulata (SNr), remains unchanged until an abrupt decrease takes place, leading to disinhibition of the superior colliculus (SC) that combines with cortical excitation to trigger a saccadic response. This nonlinearity is important for the corticostriatal pathway to produce a wide range of decision threshold levels.

Recent experiments, however, found gradual ramping of neuronal activity in the caudate (CD) nucleus before a decision threshold is reached in monkeys performing a perceptual decision task (Ding and Gold, 2010). Besides revealing an active involvement of the CD in the perceptual decision process, the observation of ramping activity also calls for generalization of the threshold modulation mechanism suggested previously (Lo and Wang, 2006). With only the direct pathway incorporated in the model, ramping activity at the CD would lead to increasing inhibition of SNr neurons, which would gradually ramp down rather than displaying a sudden drop of activity, raising the question of whether the main conclusions of Lo and Wang (2006) would still hold in that scenario.

The classical model for the BG architecture suggests that normal function requires a balance of the direct pathway, from the striatum to BG output nuclei, with the indirect pathway, which includes a reciprocal loop composed of the subthalamic nucleus (STN) and the external segment of globus pallidus (GPe; Albin et al., 1989; Hikosaka et al., 2000; Calabresi et al., 2014). The main purpose of this work is to investigate the role of the indirect

Received Aug. 28, 2014; revised Jan. 21, 2015; accepted Jan. 28, 2015.

Author contributions: W.W., J.E.R., and X.-J.W. designed research; W.W. performed research; W.W. analyzed data; W.W., J.E.R., and X.-J.W. wrote the paper.

This work was supported by a Swartz Foundation Fellowship (W.W.), the Office of Naval Research Grant N00014-13-1-0297 (X.-J.W.), the National Institutes of Health Grants R01 MH062349 (X.-J.W.) and R01 NS070865 (J.E.R.), and the National Science Foundation Division of Mathematical Sciences Award 1312508 (J.E.R.). We thank S. Fusi and C.C. Lo for early work on the computer program used in this study, and the two anonymous reviewers for suggestions in clarifying the paper.

The authors declare no competing financial interests.

Correspondence should be addressed to Xiao-Jing Wang, Center for Neural Science, New York University, 4 Washington Place, New York, NY 10003. E-mail: xjwang@nyu.edu.

DOI:10.1523/JNEUROSCI.3611-14.2015

 0270-6474/15/354052-13$15.00/0

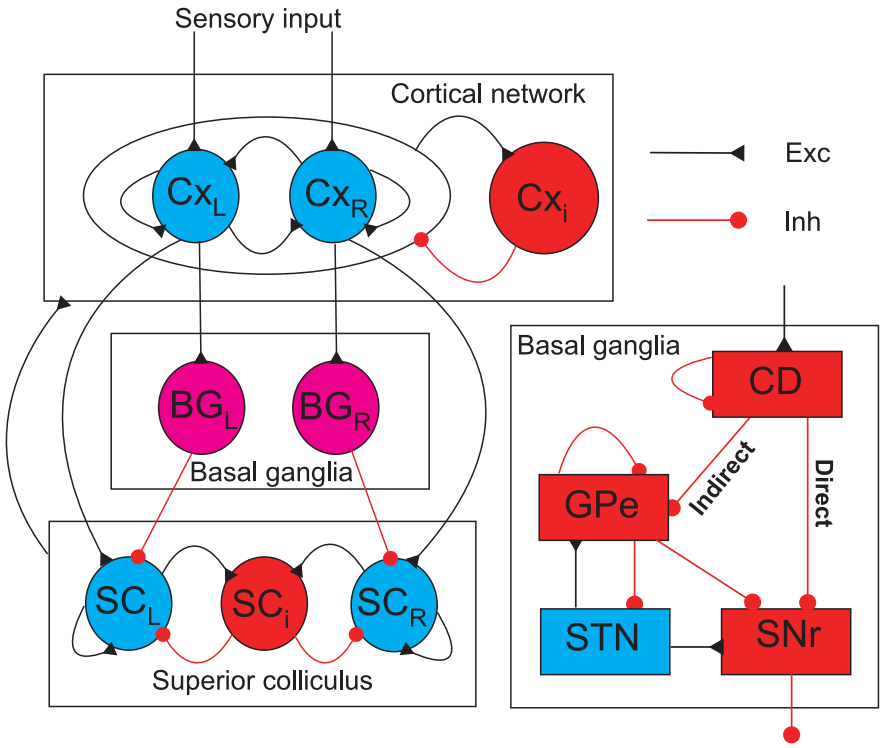

Figure 1. Schematic circuit model with three interconnected structures: the cortex, BG, and SC. The two selective excitatory populations in the cortical circuit exhibit ramping activity reflecting integration of sensory input and compete with each other through shared inhibition. Sensory evidence accumulated in the cortical network is sent to the SC (a command center for eye movement) and through the BG. The SC sends feedback signals to the cortex. Inset, The structure of the BG used in our model. Signals to the CD are transmitted to the output nucleus (SNr) through two pathways: the direct pathway (Direct) from the CD directly to the SNr and the indirect pathway (Indirect) from the CD through the GPe, STN to the SNr. Exc, Excitatory; Inh, inhibitory; subscript L, left; subscript R, right. Cx_i and SC_i are inhibitory populations in the Cx and SC, respectively.

pathway in perceptual decision making. In particular, we generalize the previous threshold detection and modulation mechanism (Lo and Wang, 2006) by developing a decision-making circuit model incorporating the indirect pathway of the BG and the experimentally observed ramping activity at the CD.

The BG are centrally implicated in parkinsonism, one important feature of which is enhanced oscillations in the population neuronal activity in a broadly defined beta band (8–30 Hz; Boraud et al., 2005; Gatev et al., 2006; Hammond et al., 2007; Obeso et al., 2008). The strong interconnections between the STN and GPe highlight the role of this subcircuit as a natural source of rhythmic BG activity (Plenz and Kital, 1999; Gillies et al., 2002; Terman et al., 2002; Holgado et al., 2010; Kumar et al., 2011). Our model suggests a circuit mechanism for the generation of beta oscillations in the STN–GPe subnetwork under experimentally identified parameter modulations, which offers novel support for the role of NMDA in this activity pattern. We investigate the influence of the resulting beta oscillations on perceptual decision-making behaviors and show that the mean reaction time and range of threshold values are significantly reduced.

Materials and Methods

Behavioral task simulation. We constructed and tested our model focusing on a widely used perceptual decision task, the random-dot visual direction discrimination task (Newsome et al., 1989; Roitman and Shadlen, 2002; Ding and Gold, 2010, 2013). In that experiment, partially coherent moving dots are presented and the subject is required to make a two-alternative choice about the coherent direction (the reaction-time version of the task). In our model simulation, the direction of coherent motion is assumed to be leftward or rightward. Two signals, representing sensory input induced by the leftward and rightward moving dots, are fed into left-preferring and right-preferring cortical modules Cx_L and Cx_R, respectively, in a model cortical network (Fig. 1). The firing times of each input neuron are sampled from a Poisson process with a mean rate μ. The mean μ depends linearly on the dot coherence level and is given by the equations $\mu_0 + \mu_A \times c$ for the preferred direction and $\mu_0 - \mu_B \times c$ for the nonpreferred direction, where μ_0 (20 Hz) is the baseline input, c (between 0 and 100%) is the coherence level, and μ_A (60 Hz) and μ_B (20 Hz) are proportionality factors (Wang, 2002). Cortical outputs project to a model SC with two excitatory projection units, SC_L and SC_R. The decision time is defined as the time interval between the start of the sensory input to the cortex and the onset of activity in an SC unit, SC_e, representing a saccadic burst, where the subscript "e" is either L or R, corresponding to the population that becomes active. The decision threshold is defined as the firing rate of the cortical population Cx_e that projects to the active SC_e unit at the onset time of SC_e activity. A correct trial is defined as a trial in which the model generates a saccadic burst in the same direction as the coherent motion. Model performance is defined as the fraction of correct trials.

Neuron model. Neurons in the STN and GPe display postinhibitory rebound (PIR) bursts, i.e., a brief burst of spikes is produced at the end of a relatively long (~100 ms) period of hyperpolarization (Bevan et al., 2002a; Kita, 2007), which is strongly enhanced in the parkinsonian state (Filion and Tremblay, 1991; Bergman et al., 1994; Boraud et al., 1998; Wichmann and Soares, 2006). We use the integrate-and-fire-or-burst model (Smith et al., 2000) to capture this firing characteristic of STN and GPe neurons. The membrane dynamics is given by the following equation (Eq. 1):

$$C\frac{dV}{dt} = -g_L(V - V_L) - g_T h H(V - V_h)(V - V_T) - I_{syn}$$

where $H(V)$ is the Heaviside step function and where $C = 0.5$ nF, $g_L = 25$ nS, $V_L = -70$ mV, $V_h = -60$ mV, and $V_T = 120$ mV. When the membrane potential reaches a boundary V_b, it is reset to V_r, where $V_b = -50$ mV and $V_r = -55$ mV. In this model, rebound burst firing is induced by a low-threshold T-type calcium current. The inactivation variable h of the current satisfies the following equations (Eqs. 2 and 3):

$$\frac{dh}{dt} = -h/\tau_h^-, \text{ when} V \geq V_h$$

and

$$\frac{dh}{dt} = (1 - h)/\tau_h^+, \text{ when} V < V_h$$

where $g_T = 60$ nS, $\tau_h^- = 20$ ms, and $\tau_h^+ = 100$ ms. For neurons in the cortex, SC, and other nuclei in the BG, we use the leaky integrate-and-fire model, which is described by Equation 1 with $g_T = 0$.

The synaptic current I_{syn} is given by the following equation (Eq. 4):

$$I_{syn} = g_1 s(V - V_E) + \frac{g_2 s(V - V_E)}{1 + e^{-0.062V/3.57}} + g_3 s(V - V_I),$$

where the reversal potentials $V_E = 0$ mV and $V_I = -70$ mV. g_k is the synaptic efficacy, where the indices $k = 1, 2, 3$ indicate AMPA, NMDA, and $GABA_A$ synapses, respectively. The gating variable s satisfies the following equations (Eqs. 5 and 6):

$$\frac{ds}{dt} = \sum_j \delta(t - t^j) - \frac{s}{\tau}$$

for AMPA and $GABA_A$ receptor-mediated currents and:

$$\frac{ds}{dt} = \alpha(1 - s)\sum_j \delta(t - t^j) - \frac{s}{\tau}$$

for NMDA receptor-mediated current, where t^j is the time for the j^{th} spike and $\alpha = 0.63$. For the decay time constant τ, we use 2 ms for AMPA, 5 ms for $GABA_A$, and 100 ms for NMDA-mediated currents. I_{syn} describes both the synaptic inputs from other neurons within the circuit and background inputs modeled as Poissonian spike trains representing sources beyond the circuit. We also use a short time delay, 0.2 ms, for synaptic transmission in both normal and parkinsonian states.

To check the possible impact of saturation of CD activity during evidence accumulation (Ding and Gold, 2010), we introduce short-term depression (STD) at corticostriatal synapses (Lovinger et al., 1993; Ding et al., 2008). The STD is implemented by including a factor D that multiplies all terms on the right side of Equation 4 (Hempel et al., 2000), which satisfies the following equation (Eq. 7):

$$\frac{dD}{dt} = -pD\sum_j \delta(t - t^j) + \frac{1 - D}{\tau_D}$$

where $p = 0.45$ and $\tau_D = 600$ ms.

Network structure. The full circuit includes three brain areas (Fig. 1): the cortical network (Cx), the BG, and the SC. The Cx performs evidence accumulation, as observed, for example, in the lateral intraparietal area and frontal eye field, and is described in previous work (Wang, 2002). The present model extends an earlier one (Lo and Wang, 2006) by including the indirect pathway of the BG, encompassing a projection from the CD (the eye movement part of the striatum) to the STN–GPe loop as well as projections from both the STN and GPe to the SNr. The SNr is the output nucleus of the BG involved in saccadic eye movements (Basso and Sommer, 2011). The projection directly from the cortex to the STN, the so-called hyperdirect pathway, is simplified to a background input to the STN.

Each BG nucleus includes two populations of neurons selective to left and right moving dots, respectively. Each population in the CD and SNr includes 250 neurons with all-to-all connections. Each population in the STN and GPe includes 2500 neurons, since we will use sparse connectivity within the STN–GPe subcircuit to prevent the population spike pattern from being oversynchronized in the parkinsonian state. Following another model (Kumar et al., 2011), the connection probabilities used are 0.05 for STN→GPe, 0.05 for GPe→GPe, and 0.02 for GPe→STN, reflecting the sparse connections between the STN and GPe and also within the GPe (Kita and Kitai, 1994; Bevan et al., 1997; Sadek et al., 2007; Baufreton et al., 2009). There are no known recurrent connections within the STN (Sato et al., 2000). Hence, such connections are not included. All other projections are all-to-all for the left and right selective populations, respectively. The SC network is described as in previous work (Lo and Wang, 2006). The SC network generates all-or-none burst activity due to strong recurrent connection there and sends feedback to the Cx, which, due to recruitment of the inhibitory population Cx_i, terminates the ramping in the cortical circuit.

The connection efficacies within the BG used in the model are the following for the normal state: $g_{CD-CD} = 1.0$ nS, $g_{CD-SNr} = 3.0$ nS, $g_{GPe-GPe} = 1.5$ nS, $g_{GPe-STN} = 0.6$ nS, $g_{GPe-SNr} = 0.08$ nS, $g^{AMPA}_{STN-GPe} = 0.05$ nS, $g^{NMDA}_{STN-GPe} = 2.0$ nS, $g_{STN-SNr} = 0.06$ nS. The efficacy of the connection from the Cx to the CD (g_{Cx-CD}) varies between 1 nS and 4.5 nS. The CD to the GPe efficacy g_{CD-GPe} varies between 0 and 8 nS. For the cortical and SC networks, we use the same synaptic connection properties as in past studies (Wang, 2002; Lo and Wang, 2006).

We also investigated how the normal state is transformed into a parkinsonian state characterized by enhanced beta oscillations. Our beta oscillations are generated within the STN–GPe subcircuit. To simulate the parkinsonian state, we update the synaptic efficacies within the STN–GPe circuit to the following values: $g_{GPe-GPe} = 0.02$ nS, $g_{GPe-STN} = 10$ nS, $g^{NMDA}_{STN-GPe} = 10$ nS (the other connection efficacies within the model are kept the same as the normal state). These updates reflect changes in strengths and numbers of connections as well as lessening of STD of GPe–STN connections resulting from the lower GPe firing rates seen experimentally with dopamine depletion (Stanford and Cooper, 1999; Ogura and Kita, 2000; Cragg et al., 2004; Shen and Johnson, 2005; Kita, 2007; Fan et al., 2012; Wilson, 2013). These and other changes in values were chosen to reproduce key effects qualitatively rather than quantitatively. They amount to a substantial increase of the excitatory–inhibitory interplay between the STN and GPe along with a reduction in the intra-GPe inhibition.

Background inputs, which are incorporated into Equation 4, are described as Poissonian spike trains. All of the BG nuclei in the model receive AMPAergic background inputs, with possible cortical and thalamic origins. GPe neurons also receive GABAergic background inputs representing additional inputs from the striatum. For normal states, the synaptic efficacies and Poisson rates used for the background inputs in our model are as follows: 4.0 nS and 0.8 kHz for the CD; 3.0 nS and 3.2 kHz for GPe AMPA receptors; 2.0 nS and 2.0 kHz for GPe $GABA_A$ receptors; 1.6 nS and 4.0 kHz for the STN; 14 nS and 0.8 kHz for the SNr. For the parkinsonion state we use 1.6 nS and 4.0 kHz for GPe AMPA receptors, 22 nS and 2.0 kHz for GPe $GABA_A$ receptors, 1.0 nS and 3.2 kHz for the STN, and keep the other values unchanged. The strongly enhanced background CD to GPe efficacy in part represents the removal of the inhibitory effect of dopamine on the striatal neurons projecting to the indirect pathway (Kish et al., 1999; Obeso et al., 2000; Kita, 2007). Furthermore, since differences in ramping CD activity during evidence accumulation between the normal and parkinsonian states have not yet been quantified, we maintain the same ramping pattern across these states and use the enhanced background CD-to-GPe efficacy to represent the overall increase in CD firing rate in the parkinsonian state. If we instead allow the rate of background inputs to increase, then a much smaller increase in CD-to-GPe efficacy yields the same results as we present here (e.g., 5 nS and 10 kHz; data not shown).

Results

Balance of the direct and indirect pathways during evidence accumulation

Previous work suggests that the corticostriatal pathway can effectively adjust the decision threshold during perceptual decision making (Lo and Wang, 2006). The mechanism involved works best in the presence of a strong nonlinearity, i.e., an abrupt suppression of SNr activity immediately before the onset of a saccadic response (presumably coinciding with the threshold crossing), which was observed in physiological recording of monkeys performing saccade tasks (Hikosaka and Wurtz, 1983; Sato and Hikosaka, 2002). With a gradual intensification of CD activity during evidence accumulation in the random-dot task (Ding and Gold, 2010), however, the direct pathway projection would cause the SNr activity to ramp down in a graded way, rather than exhibiting a sudden drop of activity just before a saccade.

By incorporating the indirect pathway as well, we find that SNr activity can remain unchanged over time during most of the CD ramping process (Fig. 2). In our simulations, ramping neuronal activity in the CD leads to a gradual decrease of GPe activity and a corresponding increase of STN activity, which cancels out the direct impact of CD output on SNr activity. This balancing effect weakens, however, when GPe activity becomes sufficiently low and disappears entirely when the GPe activity reaches zero and STN activity correspondingly plateaus. The continued rise in CD output then sharply suppresses SNr activity. In a way similar to that of the earlier model (Lo and Wang, 2006), the abrupt

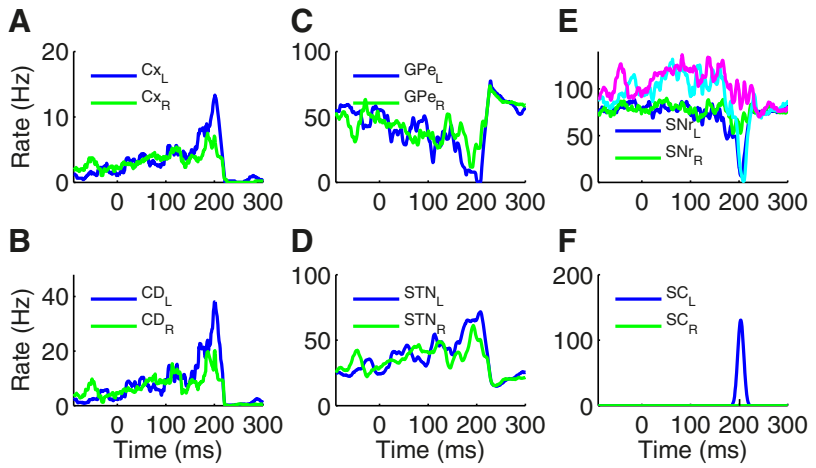

Figure 2. Behavior of the model Cx–BG–SC circuit when the indirect pathway balances with the direct pathway. ***A***, The two selective populations in the Cx compete with each other and accumulate evidence. ***B***, CD populations innervated by the Cx show ramping activity. ***C***, ***D***, GPe neurons (***C***) inhibited by CD neurons decrease their activity, while STN neurons (***D***) increase their activity due to reduced inhibition from the GPe. ***E***, The innervations from the direct and indirect pathways to the SNr neurons balance with each other, such that SNr activity remains unchanged despite the ramping in the CD (blue and green curves). When the activity of GPe neurons decreases to near zero, a continued increase of CD firing leads to further inhibition of the SNr, whose neural activity exhibits a sharp suppression. ***F***, The resulting disinhibition of SC neurons, combined with sufficient cortical excitation, eventually triggers a burst response (indicating a categorical choice) in one of the two SC neural populations (with peak activity at ~200 ms as indicated by the black bar). Ramping activity in the cortex is terminated by the feedback signal from the SC, defining a threshold for the decision process. Parameter values: $g_{Cx-CD} = 3$ nS, $g_{CD-GPe} = 4$ nS; coherence level $c = 25.6\%$. The SNr activity in the case when the indirect pathway overbalances the direct pathway, with $g_{CD-GPe} = 6$ nS, is also shown (***E***, cyan, left selective; magenta, right selective).

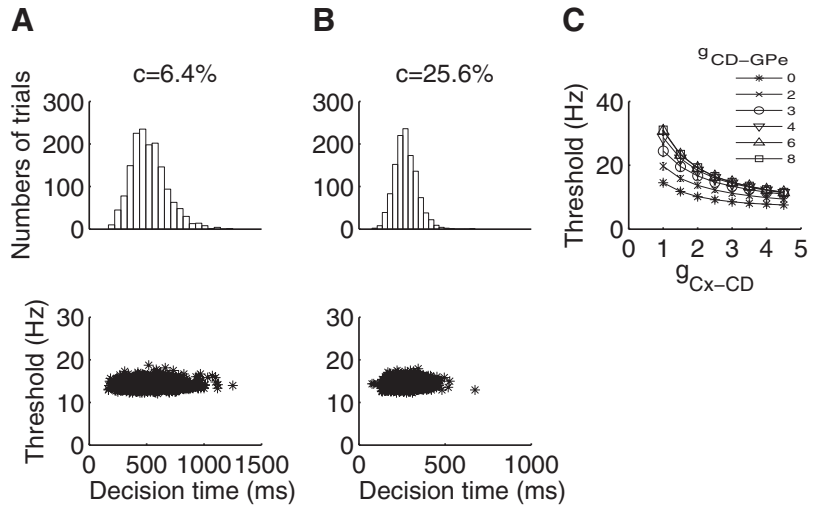

Figure 3. Decision threshold and its dependence on the strength of the indirect pathway. ***A***, ***B***, The distribution of decision times and thresholds for two motion-coherence levels. The decision time is modulated by coherence level of the stimulus (top), while the threshold is insensitive to the stimulus strength (bottom). ***C***, The dependence of threshold on the corticostriatal connection strength g_{Cx-CD} for different values of g_{CD-GPe}, the strength of the indirect pathway. Error bars indicate SD.

decline of SNr activity releases the downstream suppression of the SC, which combined with direct excitation of decision neurons in the cortex results in a burst of activity in the SC (with peak activity at 200 ms as indicated in Fig. 2*F*, in this example). The feedback from the SC to the cortex in turn recruits the inhibitory cortical population, Cx_i, which terminates the evidence accumulation process there. Thus, the extension of a previous model (Lo and Wang, 2006) to include the indirect pathway allows appropriate evidence accumulation thresholding and decision responses in the presence of more realistic neuronal activity at the striatum. We next consider how this performance depends on the network features that contribute to the balance between the direct and indirect pathway inputs to the SNr.

Impact of relative weights of the direct and indirect pathways

We find that when the coherence level of the random-dot sensory inputs is varied, the mean response time increases with the task difficulty (lower coherence), but the decision threshold, defined as the firing rate of the corresponding cortical population at the onset time of SC activity, remains the same (Fig. 3*A*,*B*). This finding extends an earlier observation (Lo and Wang, 2006) to the case when gradual evidence accumulation in the CD and the indirect pathway are included. To understand more fully the impact of the indirect pathway, we adjust certain key model parameters and investigate their effects on the decision time and threshold. Adjusting the corticostriatal efficacy, g_{Cx-CD}, can effectively modulate the decision threshold, as found previously (Lo and Wang, 2006). Without including the indirect pathway, however, adjusting g_{Cx-CD} can only change the threshold value within a narrow range when the ramping activity in the CD during evidence accumulation is taken into account (Fig. 3*C*, the $g_{CD-GPe} = 0$ case). We find that enhancing the strength of the indirect pathway by increasing g_{CD-GPe} significantly widens the range of threshold values (Fig. 3*C*). Defining this range Δ_{th} by the difference in threshold values found for g_{Cx-CD} between 1.0 and 4.5 nS, we observed a rapid increase in Δ_{th} when g_{CD-GPe} is increased from 0 (Fig. 4*A*). Moreover, Δ_{th} saturates when g_{CD-GPe} is larger than a critical value of ~4 nS (when there is a balance between the direct and indirect pathways; Fig. 2), above which the indirect pathway effectively counterbalances the direct pathway until GPe activity becomes largely suppressed.

Striatal projection neurons that mediate direct and indirect pathways express D1 and D2 receptors, respectively (Calabresi et al., 2014). We have assumed that the direct and indirect pathway CD populations have the same firing rates and have lumped them together. The CD neurons projecting through the direct pathway (expressing D1 receptors) and through the indirect pathway (expressing D2 receptors) show dissociable encoding of choice and learning, however (Hikida et al., 2010; Kravitz et al., 2012; Tai et al., 2012). To test the robustness of our decision-making mechanism, we perform additional simulations for the case when left-selective and right-selective D1-expressing and D2-expressing CD neurons have different firing rates, i.e., the CD population selective for the coherent motion direction (say, the left direction) has a higher firing rate than that selective for the right direction for D1-expressing CD neurons, while for

D2-expressing CD neurons, the CD population selective for the right has a higher firing rate than that selective for the left direction. This asymmetry of firing rates might result from reward history and, during the preparatory period, will position the subjects to access higher reward opportunities. To simulate our model in this situation, we increased the background efficacy from 4 to 5 nS for D1-expressing CD neurons selective for the left direction and D2-expressing CD neurons selective for the right direction. This introduces an asymmetry in CD firing rates. The resulting network activity resembles that of Figure 2 (data not shown). From Figure 4*B*, we see that our proposed mechanism about balance between the two pathways still holds. Note that the saturation value for g_{CD-GPe} increases to 6 from 4 nS in our original model (Fig. 4*A*), since in the present case the D2-expressing CD population selective for left has a lower rate than the rate of the D1-expressing CD population selective for left, and therefore a higher efficacy is needed to achieve balance between the two pathways. This result suggests that the mechanism we have introduced does not depend critically on the assumption that the CD populations projecting to the two pathways have the same spike rates. In the following we will not distinguish D1-expressing and D2-expressing CD neurons since it is currently unknown whether they exhibit different ramping activity during a perceptual decision process.

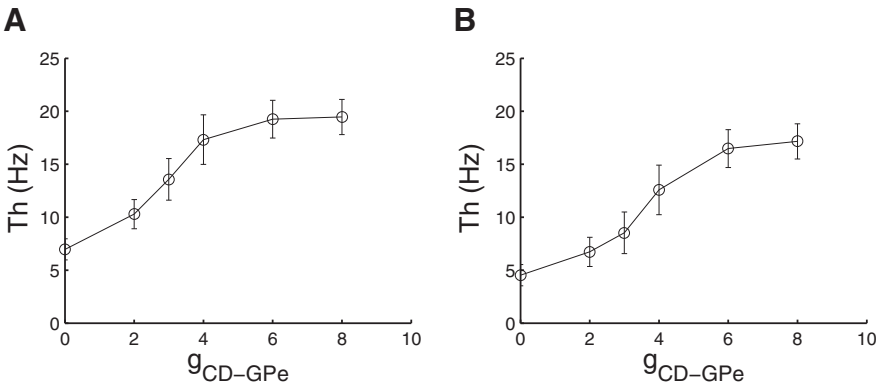

Figure 4. Dependence of range of threshold values on the strength of the indirect pathway. The range of threshold values obtained through g_{Cx-CD} modulation (Δ_{th}) is enlarged by increasing g_{CD-GPe}. ***A***, When D1-expressing and D2-expressing CD populations have the same firing rates as in Figure 2, the ramp saturates when g_{CD-GPe} exceeds 4 nS, the value for which the indirect pathway balances the direct pathway. ***B***, When D1-expressing and D2-expressing CD populations have different firing rates, the balance value for g_{CD-GPe} increases to 6 nS, since in the present case the D2-expressing CD population selective for motion direction has a lower rate than that of the D1-expressing CD population, and therefore a higher efficacy is needed to achieve balance between the two pathways. Error bars indicate SD.

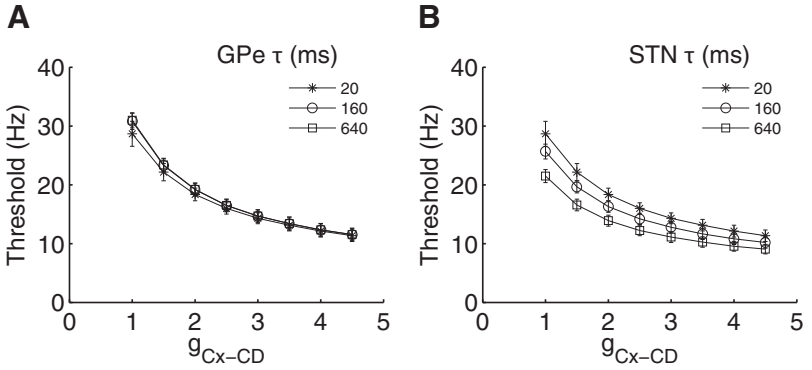

Figure 5. Impact of slowing down the membrane dynamics of indirect pathway nuclei on threshold modulation by corticostriatal efficacy. ***A***, The dependence on corticostriatal connection strength g_{Cx-CD} for different GPe membrane time constants. The time constant $\tau = C/g_L$ is slowed by increasing the capacitance C with a fixing leak conductance g_L. Three time constants are compared, with $\tau = 20$ ms representing the normal time constant of GPe neurons. The threshold is insensitive to the slowing down of GPe membrane dynamics. ***B***, Same as ***A***, but for the STN. $\tau = 20$ ms is the normal time constant of STN neurons. When the STN membrane dynamics are slowed down, the threshold is decreased and its range is reduced.

One possible test of the pathway balancing that we propose would come from localized cooling of particular BG areas, to the point where neuronal responses are slowed but not inactivated (Long and Fee, 2008). Simulations of such cooling in our model, implemented by increasing the neuronal membrane time constant, reveal different effects, depending on the modulated target. Cooling of the GPe has little impact on the balance between pathways, resulting in little change in threshold for particular g_{Cx-CD} values and in the overall range of response thresholds (Fig. 5*A*). In contrast, cooling of the STN weakens the ability of its outputs to counterbalance direct pathway activity. This change results in lowered thresholds over all g_{Cx-CD} values as well as a diminished range of response thresholds (Fig. 5*B*). These alterations and differences between nuclei represent predictions for future experimental investigation.

In our model, the performance and mean decision time (defined as the time lapse from stimulus initiation to threshold crossing) are also influenced by g_{CD-GPe} (Fig. 6). Specifically, when the relative weight of the indirect pathway is enhanced by increasing g_{CD-GPe} from 0 to the balancing value 4 nS, performance improves and response time increases across a wide range of stimulus coherence levels; that is, accuracy is favored over speed. Increasing g_{CD-GPe} even higher, from 4 to 6 nS, yields no change of the performance and mean decision time, consistent with the observation that the decision threshold becomes insensitive to g_{CD-GPe} in this regime of indirect pathway predominance.

The activity of CD neurons was observed to eventually saturate during evidence accumulation (Ding and Gold, 2010). One way to introduce saturation for CD activity is through the inclusion of STD at corticostriatal synapses. Figure 7*A* illustrates the mean activation level of AMPAergic synapses with STD receiving a linear ramping presynaptic input. The synaptic activation level Ds, where D and s are shown in the middle panels of Figure 7*A*, reaches a plateau (Fig. 7*A*, bottom) depending on the slope of ramping input (Fig. 7*A*, top). CD activity thus saturates in our circuit model when there is STD at corticostriatal synapses (Fig. 7*B*). The ramping in the Cx (Fig. 7*B*, top) leads to a saturation of the activation level of AMPAergic corticostriatal synapses (Fig. 7*B*, middle), and therefore a saturation of the CD activity (Fig. 7*B*, bottom). Note that now the input strength to the SNr is weakened due to the CD saturation, and SNr activity remains very high, which would lead to a failure of disinhibition before saccade onset and prolong the decision time. Simply doubling the synaptic efficacies along both the direct and indirect pathways, however, restores the action selection mechanism and the dependence of

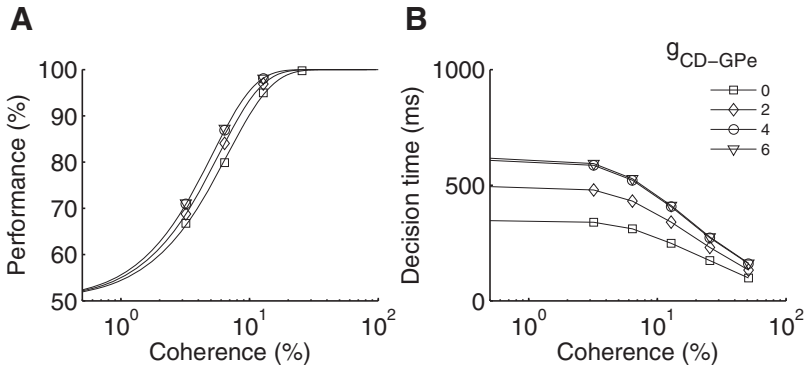

Figure 6. Effect of pathway balance on decision making. ***A***, ***B***, Performance (***A***; proportion of trials for correct response) and mean decision time (***B***) as a function of stimulus coherence level, with four different g_{CD-GPe} values ($g_{Cx-CD} = 3$ nS). With the strengthening of the input to the indirect pathway, the performance is enhanced, while the decision time is also increased. When the indirect pathway balances or overweights the direct pathway, the performance and mean decision time become saturated (curves with circles and triangles are indistinguishable).

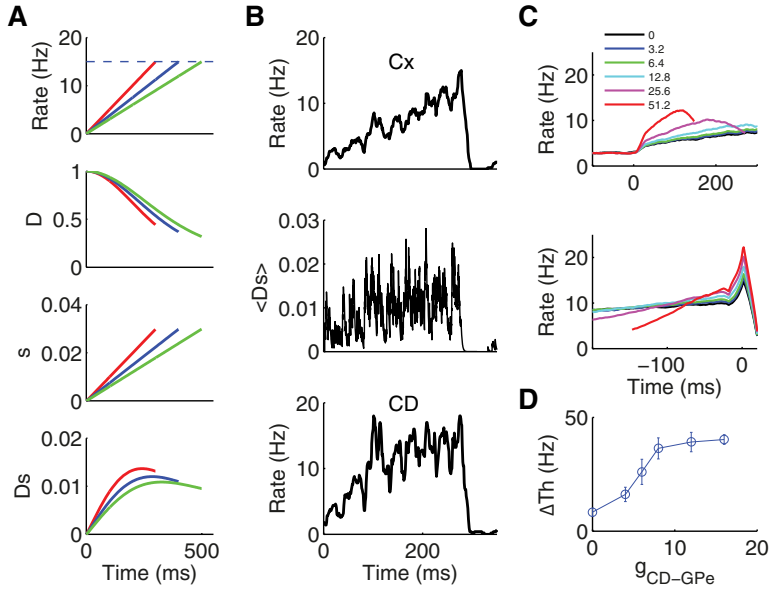

Figure 7. Decision threshold and its dependence on the strength of the indirect pathway with CD activity saturation. ***A***, Illustration of activation level saturation of an AMPAergic synapse with STD. Top, Linearly ramping presynaptic input rates. Three colored lines correspond to three ramping slopes. Middle, Depression factor D and AMPAergic synaptic gating variable s as a function of time, obtained from Equations 7 and 5 by replacing $\sum_j \delta(t - t^j)$ with a population-averaged input rate as shown in the top panel. Bottom, The activation level of an AMPAergic synapse with depression, Ds, shows a saturation depending on the slope of the ramping input. ***B***, Cx and CD activities with the inclusion of STD at corticostriatal synapses in the circuit model. Top, Ramping Cx activity. Middle, Averaged individual AMPAergic synaptic activation level shows a saturation, where $Ds = \sum_i D_i s_i / N_{Cx}$ with N_{Cx} representing the number of neurons in a selective Cx population. Bottom, CD firing rate saturates when the Cx ramps up. ***C***, CD activity for six coherence levels each averaged over 800 trials shows saturation when the activity levels for different trials are aligned with stimulus onset (top) and saccade onset (bottom). ***D***, The range of threshold values, Δ_{th}, shows a similar dependence on g_{CD-GPe} as that for original model (compare with Fig. 4*A*), and saturates when g_{CD-GPe} exceeds 8 nS, the value at which the indirect pathway balances the direct pathway in this case. Error bars indicate SD. Note that the synaptic efficacies along the direct and indirect pathways are doubled to achieve a disinhibition at the SNr before saccade onset despite CD saturation. In ***B*** and ***D***, the coherence level is 25.6%. In ***B*** and ***C***, $g_{Cx-CD} = 3$ nS and $g_{CD-GPe} = 8$ nS.

threshold on g_{CD-GPe}. The saturation of the ensemble-averaged CD activity when aligned with stimulus onset (top) and saccade onset (bottom) are shown in Figure 7*C* for several stimulus coherence values. The range of threshold values, Δ_{th}, as a function of g_{CD-GPe} (Fig. 7*D*) again shows a two-phase behavior (rapid increase followed by a saturation), resembling that for the original model (Fig. 4*A*). The critical value of g_{CD-GPe}, above which the indirect pathway balances with the direct pathway, shifts to ~8 nS now, corresponding to the doubling of efficacies along the direct and indirect pathways. Therefore, taking into account CD saturation does not impair the mechanism that we have introduced for effective threshold modulation.

Beta oscillations generated in the STN–GPe subcircuit

Enhanced beta-band oscillations in neuronal population activity in the BG represent one characteristic feature of parkinsonism, which is associated with dopamine depletion in the BG (Boraud et al., 2005; Hammond et al., 2007; Rubin et al., 2012; Calabresi et al., 2014). We investigated how experimentally observed changes induced by dopamine depletion might alter the model behavior, in particular considering the effects of (1) enhanced synaptic connections between STN and GPe neurons (Cragg et al., 2004; Shen and Johnson, 2005; Kita, 2007; Fan et al., 2012; Wilson, 2013), including the STN-to-GPe excitation mediated by NMDA receptors (Bernard and Bolam, 1998; Kita et al., 2004), and (2) enhanced efficacy of the striatal GABAergic projection to the GPe (Kish et al., 1999; Obeso et al., 2000; Kita, 2007).

With appropriate parameter changes reflecting these conditions, the STN–GPe subcircuit of our model gives rise to synchronized firing at a frequency within the beta band (Fig. 8). In this regime, the collective population activity shows an oscillatory pattern (Fig. 8*C*), with a rhythmic frequency of ~16 Hz (Fig. 8*D*). Both STN and GPe neurons exhibit bursts of spikes and also a small proportion of tonic spikes (Fig. 8*A*,*B*), emulating the enhanced bursting that can arise in these neurons in parkinsonism (Filion and Tremblay, 1991; Bergman et al., 1994; Wichmann and Soares, 2006). This bursting in our model STN and GPe cells results from their intrinsic PIR property (a depolarizing potential that takes place following prolonged hyperpolarization; Selverston and Moulins, 1985; Llinás, 1988; Getting, 1989; Destexhe and Sejnowski, 2003). In contrast to irregular tonic spiking observed in STN and GPe neurons with control parameter values (Fig. 2, except the rebound bursts of GPe neurons after saccade initiation), enhanced inhibition from the striatum to the GPe and from the GPe to the STN in the model provides the prolonged hyperpolarization necessary for the generation of burst discharges in STN and GPe neurons. Once the T current is available to support PIR, excitatory inputs from the STN can induce bursting in the GPe and excitatory background inputs can help trigger bursting in the STN. While the extent of bursting in our model is exaggerated relative to most experimental

conditions, our results nonetheless support the idea that changes in effective connectivity properties associated with parkinsonian conditions can give rise to both beta oscillations, through altered network interactions, and increased bursting, through enhanced recruitment of intrinsic currents.

Parameter dependence of beta oscillations and oscillation frequency

Intuitively, the oscillatory periodicity of ~60 ms arises from the cyclic interplay between NMDA receptor-mediated STN-to-GPe excitation and $GABA_A$ receptor-mediated GPe-to-STN inhibition. To better quantify the dependence of the emergence of population oscillations on network properties, we systematically varied several key model parameters. In Figure 9, the effects of varying strengths of connections between the STN and GPe and of background inputs are considered. These variations reveal the parameter regime where the network exhibits beta oscillations (Fig. 9*A*, top, pale blue region), on which we focus our further analysis. Furthermore, the frequency of beta oscillations is the same in the STN and GPe, reflecting the network-based mechanism underlying this activity. Within the beta oscillation regime, increasing $g_{\mathrm{GPe-STN}}$ has little effect on STN firing rate but causes the coefficient of variation (CV) of STN firing to increase. In contrast, increasing $g^{\mathrm{NMDA}}_{\mathrm{STN-GPe}}$ strongly decreases the STN firing rate. Together, these two parameters control the GPe firing rate, suggesting that changes in one of these efficacies can counterbalance the other in terms of their influence on this property. Overall, increases in GPe firing do accompany decreases in STN firing rate, because more sustained GPe inhibition provides fewer opportunities for STN bursting.

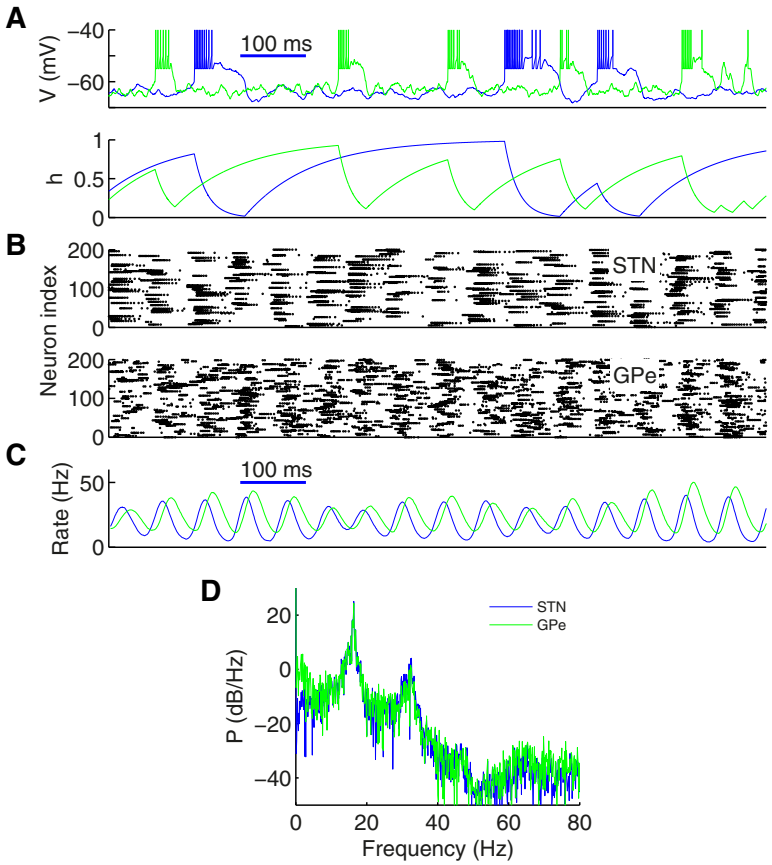

Figure 8. Beta oscillations in the isolated STN–GPe subcircuit. ***A***, Representative time courses of individual model STN (blue) and GPe (green) neurons. ***B***, Raster plots of model STN (top) and GPe (bottom) neurons (200 neurons of each type). Both STN and GPe neurons exhibit bursting activity, as observed experimentally. ***C***, Population firing rates of STN and GPe neurons. ***D***, Power spectrum of STN and GPe population firing activity, showing a peak around 16 Hz. The prominent beta-range oscillations take place when the $GABA_A$ receptor-mediated GPe-to-STN inhibition and NMDA receptor-mediated STN-to-GPe excitation are substantially increased from the control parameter set (see Materials and Methods).

The GABAergic input from the striatum to the GPe has been suggested to play an important role in determining the oscillation properties in the STN–GPe subcircuit (Terman et al., 2002; Kumar et al., 2011). Our model supports this idea and shows that the background inhibitory input to the GPe, representing input from the striatum and modeled as a background GABAergic synapse with efficacy g_{GPe_b} needs to be much stronger than in the normal state for the emergence of beta oscillations (Fig. 2, 2 nS; Fig. 8, 22 nS). Furthermore, we find that the excitatory input to the STN, representing input from the cortex and thalamus and modeled as a background AMPAergic synapse with efficacy g_{STN_b} in our model, can effectively modulate the oscillation frequency within the beta band (high-CV regimes in Fig. 9*B*, top, ranging from pale blue to yellow). Note that when either $g_{\mathrm{STN_b}}$ or $g_{\mathrm{GPe_b}}$ becomes very large, the oscillation is effectively abolished (indicated by a very low CV in Fig. 9*B*, bottom). When g_{GPe_b} is fixed and g_{STN_b} becomes large (Fig. 9*B*, top, red regime), the beta oscillation is abolished through a step-like transition from an oscillatory state to an asynchronous state. This transition is induced by the sudden loss of bursting capability in GPe neurons (from bursting dominant to tonic firing dominant) when the excitatory input from the STN becomes too strong, preventing recruitment of the low-threshold T-type calcium current. On the contrary, when $g_{\mathrm{STN_b}}$ is fixed (say, 0.8 nS) and $g_{\mathrm{GPe_b}}$ becomes large (the sector with CV above baseline in Fig. 9*B*, bottom), the CV decreases gradually as the firing of networks becomes more and more asynchronous, reflecting the stronger random inhibition. The increase of striatal input also decreases the GPe firing rate and correspondingly allows the STN to fire more rapidly (Fig. 9*B*, middle). The vertical bar in the middle panel of Figure 9*B* represents a regime where GPe neurons show a mixture of bursts and tonic spikes and STN neurons are silent.

We also investigated the influence of the longest time constants in the network and some other synaptic efficacies on the oscillation properties (Fig. 10). There are three long time constants in our STN–GPe circuit: the NMDA receptor decay time constant, τ_{NMDA}, and the recovery time constants of the inactivation variables of the T-type calcium currents responsible for PIR in the STN and GPe, τ_h^+ (STN) and τ_h^+ (GPe), respectively. We see that the oscillation frequencies are insensitive to any individual variation of these long time constants within a wide range, although they have a moderate influence on the firing rates and CVs in the STN and GPe (Fig. 10*A–C*). A step-like transition occurs when τ_h^+ (GPe) is larger than a critical value (Fig. 10*C*), induced by a sudden loss of bursting capability of GPe neurons

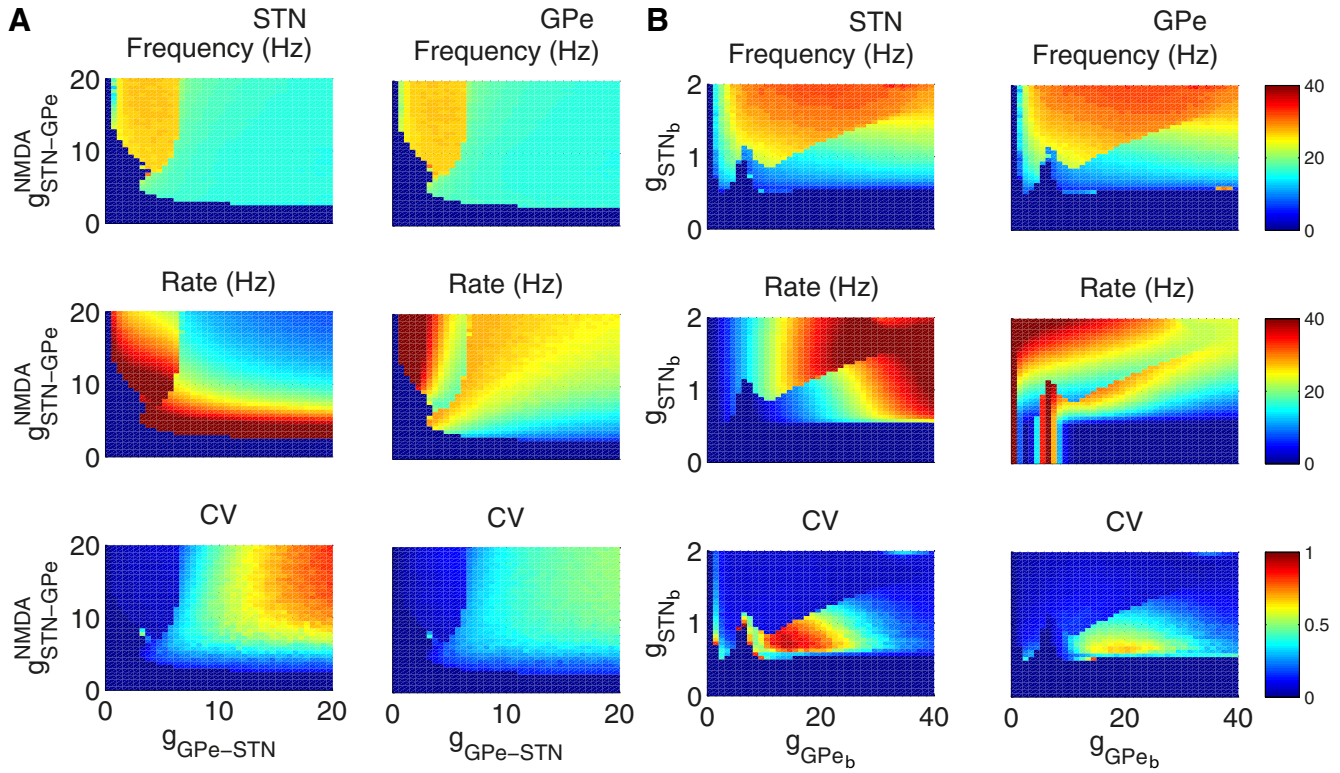

Figure 9. Dependence of the STN–GPe subcircuit behavior on the interconnection efficacies between the STN and GPe and the background inputs. ***A***, Population oscillation frequency, mean neuronal firing rate, and CV for activity of STN neurons (left column) and GPe neurons (right column) as a function of interconnection strengths $g_{GPe-STN}$ and $g^{NMDA}_{STN-GPe}$. Beta-band oscillations are robust over a broad parameter regime. ***B***, Oscillation frequency, firing rate, and CV of STN neurons (left column) and GPe neurons (right column) as a function of the strength of inhibitory background input to GPe neurons (g_{GPe_b}) and excitatory background input to STN neurons (g_{STN_b}). In an intermediate range of g_{GPe_b} values, CV is large (>0.5; bottom) and the oscillation frequency is in the beta range (~8–20 Hz; top) for a wide range of g_{GPe_b} values. Note that for the yellow regime in the top panels in ***A***, and the red regime in the top panels in ***B***, the CV is very low, and hence we do not consider these as representative of parkinsonian conditions. In determining the population oscillation frequency, we use the autocorrelation function of the population firing rate to estimate the oscillation period *T*, and the corresponding frequency is given by 1/*T*.

when the recovery of the T-type current in the GPe takes so long that it consistently is interrupted by the excitatory input from the STN, which pulls the GPe neurons out of the bursting regime. The synaptic pathway from the STN to the GPe is mediated through both NMDA and AMPA receptors (Kita et al., 2004). We already showed that when the NMDA component of coupling between the two nuclei is strong, beta oscillations can emerge and persist over a large parameter regime (Fig. 9*A*,*B*). The AMPAergic synapse does not influence the oscillation properties when the efficacy is kept at a low level (<1 nS here; Fig. 10*D*). But if the AMPA strength exceeds a critical value, the beta oscillation is sharply abolished as indicated by a very low CV. This step-like transition occurs when the pulse-like AMPAergic input from the STN is strong enough to interrupt the recovery of the T-type current in the GPe, similarly to the step in Figure 10*C*. Our model therefore suggests that in the parkinsonian state, the presence of enhanced beta oscillations signifies that the potentiation of the STN-to-GPe projection is predominantly mediated through the NMDAergic synapses.

The recurrent connection strength within the GPe, $g_{GPe-GPe}$, weakly affects the oscillation frequency and firing rate but can more strongly and gradually reduce CV (Fig. 10*E*). To have a relative large CV in our model, $g_{GPe-GPe}$ needs to be weak (in Figs. 2 and 8, the values of $g_{GPe-GPe}$ used are 1.5 and 0.02 nS, respectively). Recurrent connections within the GPe may be weakened under parkinsonian conditions (Stanford and Cooper, 1999; Ogura and Kita, 2000), but there is conflicting evidence (Miguelez et al., 2012).

Impact of beta oscillations on perceptual decision making

Now we consider the full network model in a parkinsonian state characterized by strong beta oscillations originating in the STN–GPe subcircuit (Fig. 11). Note that when the STN–GPe subcircuit is put back into the full circuit, the GPe receives both background inhibition from the CD and inhibition from the selective populations in the CD and exhibits beta oscillations over a larger parameter regime than in the isolated subcircuit (data not shown). In a simulation of perceptual decision making, neural activity in the Cx and CD modules does not change from the simulated normal state to the parkinsonian one, by the design of the model (compare Figs. 11*A*,*B*, 2*A*,*B*). The firing rates of the STN and GPe, on the other hand, now oscillate (compare Figs. 11*C*,*D*, 2*C*,*D*). In the presence of this beta oscillation, as CD activity ramps up over time, the population activity of GPe neurons maintains its oscillatory activity and appears to be insensitive to the CD ramping (Fig. 11*C*). Oscillations in the STN–GPe subcircuit are transmitted to the SNr (Fig. 11*E*), and the lack of GPe response to ramping in the CD translates into a loss of the ability of the indirect pathway to balance the direct pathway. Troughs in STN output provide repeated windows of opportunity for the direct pathway to suppress the SNr and allow an SC response (with peak activity at 180 ms, indicated by the black bar in Fig. 11*F*, in this example).

As a result, both the decision time and threshold drop substantially in the presence of beta oscillations (Fig. 12). Furthermore, there is a strong reduction in the range of threshold values

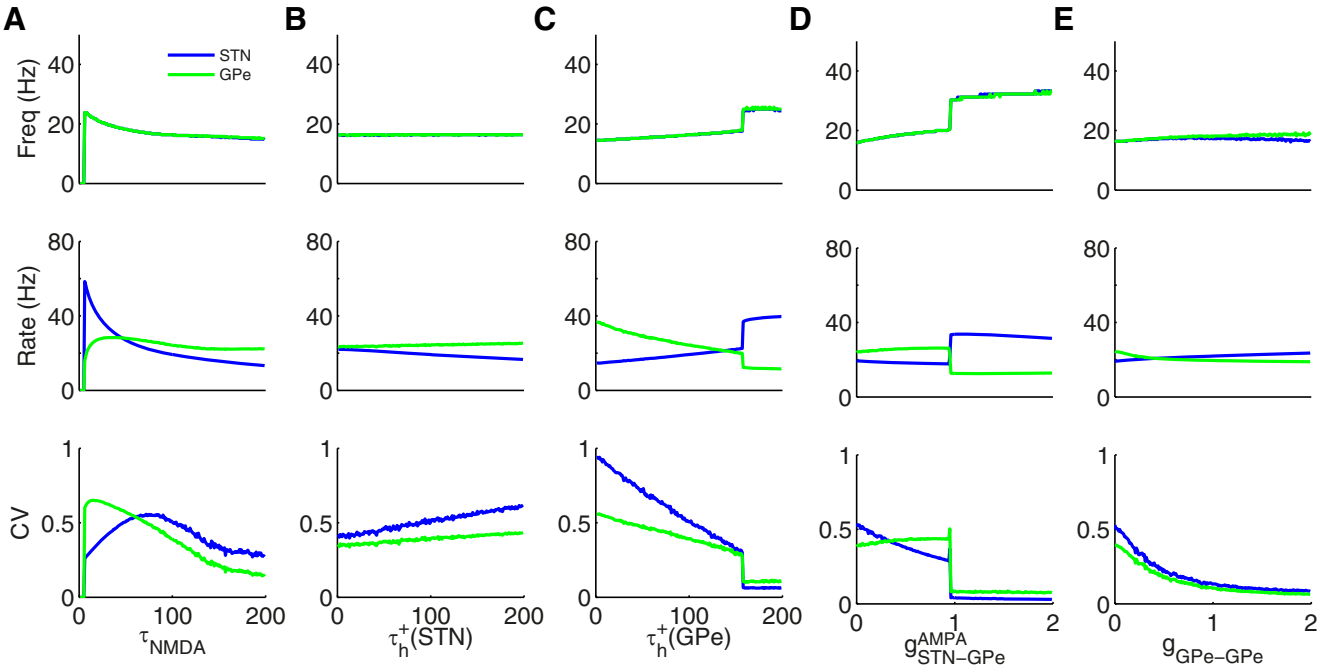

Figure 10. Parameter dependence of beta oscillations. ***A–E***, Dependence of population oscillation frequency (top), mean neuronal firing rate (middle), and CV (bottom) on the decay constant of the NMDA receptors in the excitatory synaptic projection from the STN to the GPe (***A***), the slow time constant τ_h^+ of the intrinsic T-type calcium current responsible for PIR in STN neurons (***B***) and GPe neurons (***C***), the efficacy of AMPAergic synapses from the STN to the GPe (***D***), and the strength of recurrent inhibition within the GPe (***E***). The beta oscillation frequency is insensitive to the exact values of the long time constants (***A–C***). The step-like reduction of CV in ***C*** and ***D*** corresponds to a transition from an oscillatory state to an asynchronous state. These transitions are induced by the loss of bursting of GPe neurons due to either an overly long recovery time for PIR (***C***) or an interruption of the recovery of PIR by an overly strong pulse-like AMPAergic postsynaptic current. An increase of the strength of intra-GPe inhibition significantly reduces CV during beta oscillations (***E***).

for the parkinsonian state (Fig. 12*C*,*D*), likely because even with increases in g_{Cx-CD}, the lack of sensitivity of the beta oscillations to the CD ramping means that qualitatively similar troughs of STN output occur during beta oscillations, again leading to windows of opportunity for disinhibition of SC neurons. Indeed, we find that the decision threshold in simulated parkinsonian states is quite insensitive to beta oscillation frequency, because for all frequencies, repeated epochs arise in which indirect pathway outputs fail to balance the direct pathway (Fig. 12*C*,*D*). The speeding up of decision time and loss of threshold variability that we observe are consistent with the accelerated responses observed in parkinsonism using a probabilistic selection task (Frank et al., 2007) and a cognitive task-switching task (Rowe et al., 2008), relative to the control state, and suggest that responses will be less flexible as well, which has been observed previously for Parkinson's disease patients untreated or in the off-medication state in tasks using different cognitive functions (Cools et al., 2001; Monchi et al., 2004).

Discussion

In this work, we extended a cortico-BG-SC model for threshold detection and modulation (Lo and Wang, 2006) by including the indirect pathway of the BG. Our extended model reproduces the recently observed ramping of CD activity during evidence accumulation in perceptual decision making (Ding and Gold, 2010). The main findings are twofold. First, when the indirect pathway balances the direct pathway, the decision threshold can be modulated by the corticostriatal coupling strength over a wide range, which could be important for flexibly tuning the decision threshold in a speed–accuracy tradeoff. Including STD at corticostriatal synapses in the model reproduces the saturation of CD activity during evidence accumulation (Ding and Gold, 2010) and suggests that the mechanism for threshold modulation still holds when CD activity saturates. Second, we suggest a prominent role for NMDA in generating synchronous beta oscillations that arise in the STN–GPe subnetwork under conditions associated with dopamine depletion, and we predict that in the presence of these oscillations, perceptual decision making becomes more impulsive and less flexible (cf. Cools et al., 2001; Monchi et al., 2004; Frank et al., 2007; Rowe et al., 2008; Milenkova et al., 2011).

A novel feature of our perceptual decision-making model is its emphasis on the GPe contribution to indirect pathway activity. Our model predicts that GPe activity decreases gradually toward zero during evidence accumulation, and the lower bound imposed by the zero activity level provides the nonlinearity needed for a sharp suppression of SNr activity before saccade initiation. This idea could be tested, for example, by unit recordings of GPe neurons in monkeys performing random-dot tasks. Our simulations also predict differential results from slowing time constants of neurons in the GPe and STN, such as by localized cooling that avoids complete inactivation (Long and Fee, 2008). The GPe has previously been suggested to be essential in action selection (Gurney et al., 2001a, b; Frank, 2006; Long and Fee, 2008). In our model, STN activity balances direct inhibition from the CD to the SNr, both delaying reaction time until sufficient evidence has been accumulated and suppressing selection of alternative options. The latter is consistent with a spiking version of an action selection model in which diffuse excitation from the STN to the SNr helps support firing of SNr neurons in nonselected channels; there, however, the STN does not delay direct pathway suppression of the selected SNr channel (Humphries et al., 2006). In the context of decision making, several past works showed an increase or phase shift in STN activity in high-conflict situations

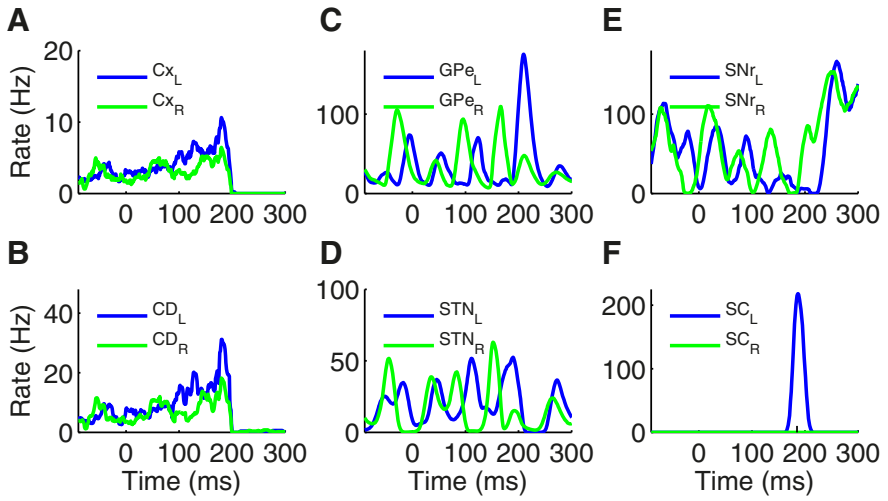

Figure 11. Decision-making behavior of the full circuit in the simulated parkinsonian state. ***A***, ***B***, Neurons in the Cx (***A***) and CD (***B***) show ramping activity, which is similar to the normal case (Fig. 2). ***C–E***, GPe (***C***) and STN (***D***) neurons exhibit strong beta-range oscillatory activity, which is transmitted to the SNr (***E***). ***F***, When the Cx activity is increased to a sufficiently large level and an oscillation results in transient SNr suppression, SC neurons produce a burst of spikes (with peak activity at ~180 ms as indicated by the black bar) and terminate the ramping activity in the Cx. Parameter values: $g_{Cx-CD} = 3$ nS, $g_{CD-GPe} = 4$ nS, coherence level $c =$ 25.6%.

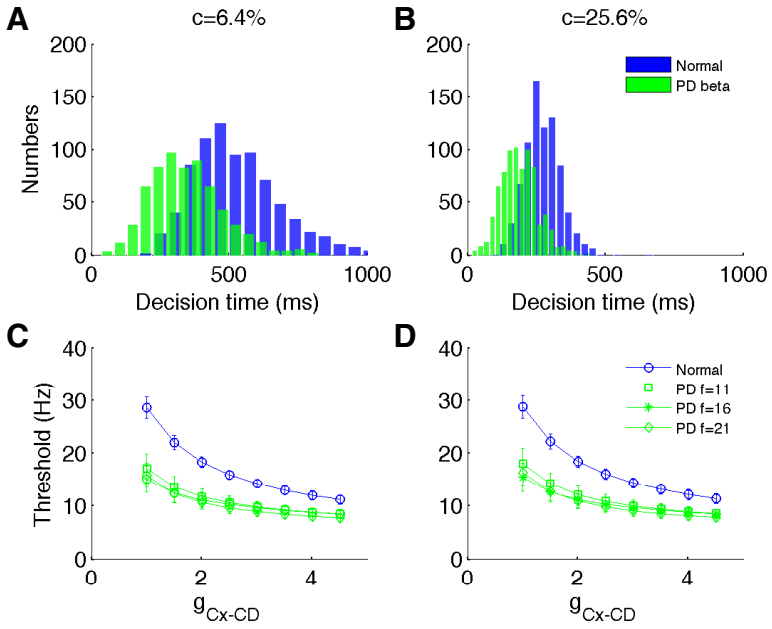

Figure 12. Reaction time distribution and range of threshold values in the parkinsonian state compared with the balanced normal state. ***A***, ***B***, Reaction-time distribution in the parkinsonian state (green, beta oscillation frequency $f = 16$ Hz) compared with the normal state (blue). ***C***, ***D***, Threshold variation as a function of the connection efficacy g_{Cx-CD} for the normal state (blue) and parkinsonian states with three oscillation frequencies: $f = 11$, 16, 21 Hz (green). ***A***, ***C***, Coherence level $c = 6.4\%$; ***B***, ***D***, Coherence level $c = 25.6\%$. The decision time is reduced for the parkinsonian state compared with the normal state (***A***, ***B***), as observed in perceptual decision making in parkinsonism. The range of threshold values is also reduced for the parkinsonian state compared with the normal state (***C***, ***D***), predicting a loss of flexibility in parkinsonism. The range of threshold values is insensitive to the exact oscillation frequency within the beta band (***C***, ***D***). In ***C*** and ***D***, the background GABAergic conductance to the STN, g_{STN_b}, is tuned to obtain three oscillation frequencies, with $g_{STN_b} = 0.7$, 1.0, and 2.0 nS, corresponding to $f = 11$, 16, and 21 Hz, respectively (compare Fig. 9). For the normal and parkinsonian states, $g_{CD-GPe} = 4$ nS. In ***A*** and ***B***, $g_{Cx-CD} = 3$ nS.

(Frank, 2006; Cavanagh et al., 2011; Ratcliff and Frank, 2012; Wiecki and Frank, 2013; Zavala et al., 2013, 2014), possibly due to cortical hyperdirect pathway inputs (cf. Hikosaka and Isoda, 2010). In our model, an increased threshold results from decreased gain of signals from cortex to striatum, and modulations of STN activity, such as by the hyperdirect pathway, could act in addition to this effect, either in a sustained way or to provide rapid decision suppression in response to incongruent information, representing a topic for future work.

The ramping of CD activity following a visual cue may be accompanied by either decreasing or increasing SNr firing rates when monkeys perform a memory-guided saccade task with only one direction rewarded (Sato and Hikosaka, 2002). Our model suggests that these two types of activity patterns might arise when the direct and indirect pathways are balanced and when the indirect pathway overbalances the direct pathway (Fig. 2*E*, cyan and magenta curves), respectively. The SNr responses could be connected to ramping dopamine signals (Kawagoe et al., 1998, 2004; Hikosaka, 2007), whereas in our model ramping at the CD has a different origin, reflecting a cortical information accumulation process. Ramping striatal activity due to reward accumulation has also been reproduced previously (Ratcliff and Frank, 2012).

Reward-dependent plasticity in the BGs is a form of reinforcement learning that can be incorporated in our model in future research to provide a more realistic implementation of the differential modulation of firing rates of direct and indirect pathway CD neurons by probability of reward, as in Figure 4*B*. Indeed, an extension of the model with only the direct pathway (Lo and Wang, 2006) that incorporates the dopamine system and reward-dependent plasticity at corticostriatal projections was recently presented (Hsiao and Lo, 2013). Related existing work includes a cortex–BG model implementing optimal decision making for multiple choices (Bogacz and Gurney, 2007) and reinforcement learning (Bogacz and Larsen, 2011) and an extended actor–critic model providing a unified description of reinforcement learning and choice incentive, where the direct and indirect pathway striatal neurons play the roles of two opponent actors and exhibit reward-dependent learning (Collins and Frank, 2014).

The indirect pathway of the BGs is strongly implicated in parkinsonism (Rubin et al., 2012). Parkinsonism is typically associated with delayed motor behaviors; however, experimental results on reaction times of Parkinson's disease patients performing cognitive tasks are highly variable (Robert et al., 2009). These include the observation of decreased reaction times for Parkinson's disease patients off dopamine medication performing a probabilistic selection task (Frank et al., 2007) and a cognitive task-switching task (Rowe et al., 2008), compared with

normal subjects, and also the finding that reaction times decrease with STN deep brain stimulation, consistent with the idea that STN modulates decision thresholds (Cavanagh et al., 2011; Green et al., 2013; Frank et al., 2015). In a regime with beta oscillations, our model predicts a reduced decision time for untreated Parkinson's disease subjects performing perceptual decision making. Furthermore, in this regime in our simulations, the range of possible decision thresholds is limited, which predicts that a decreased response flexibility will accompany the reaction-time change, reminiscent of the loss of cognitive flexibility for untreated Parkinson's disease patients in tasks using different cognitive functions (Cools et al., 2001; Monchi et al., 2004). It remains for future work to determine how changes in STN activity would alter decision thresholds in the parkinsonian regime in our model.

Several models about the origins of rhythmic activity, such as beta-band oscillations in parkinsonism, have been proposed, emphasizing the STN–GPe circuit (Terman et al., 2002; Holgado et al., 2010; Kumar et al., 2011; Park et al., 2011; Pavlides et al., 2012), the hyperdirect pathway (Leblois et al., 2006), the striatum (McCarthy et al., 2011), and the cortex (Silberstein et al., 2005; Roopun et al., 2008; Lee et al., 2013). The reciprocal interactions between the STN and GPe provide a natural substrate for rhythm generation (Plenz and Kital, 1999; Bevan et al., 2002b; Terman et al., 2002; Mallet et al., 2008; Tachibana et al., 2011). Explorations of possible mechanisms for beta oscillation rhythmogenesis in the STN–GPe circuit typically involve changes in connection strengths between the STN and GPe or within the GPe, relative to nonoscillatory conditions (Holgado et al., 2010). Our model predicts that potentiated STN-to-GPe connections in parkinsonism are predominantly mediated through NMDA receptors, which can be tested experimentally and used to differentiate this work from previous models. Subunit-specific NMDA antagonists have been found to have antiparkinsonian actions on both motor (Steece-Collier et al., 2000; Löschmann et al., 2004) and cognitive (Hsieh et al., 2012) dysfunctions in animal models of parkinsonism, and the injection of NMDA antagonists directly into the medial pallidum of parkinsonian monkeys has been shown to reverse movement-related symptoms (Graham et al., 1990; Mitchell and Carroll, 1997). Furthermore, consistent with previous work emphasizing the importance of inhibitory input to the GPe (Terman et al., 2002; Kumar et al., 2011), we found that the GABAergic input from the striatum to the GPe, and the excitatory input from the cortex and thalamus to the STN, can modulate oscillation frequencies within the beta band. Importantly, the impact of beta oscillations on perceptual decision making that we demonstrate is independent of the mechanism underlying beta oscillations and would apply even if the beta oscillations were transmitted from a cortical source.

We assume that CD activity in the parkinsonian and normal states is the same, which obviously oversimplifies the neurological changes associated with parkinsonism. The present model can readily incorporate more realistic representations of striatal activity during perceptual decision making for both normal and parkinsonian states when relevant measurements become available. Recently, it was found that the globus pallidus (GP) of rats (homolog of the GPe of primates) is composed of two distinct groups of neurons (Mallet et al., 2008, 2012; Nevado-Holgado et al., 2014), and it would also be of interest to include both types and explore their roles in decision making. Another extension would be the addition of the thalamus to form a complete, spiking cortico-basal ganglia-thalamic loop model. Meanwhile, in its current form, our model suggests novel mechanisms, which should be amenable to future experimental testing, for flexible perceptual decision making in the presence of ramping striatal activity and for how this decision making may be perturbed under the influence of indirect pathway beta oscillations.

References

Albin RL, Young AB, Penney JB (1989) The functional anatomy of basal ganglia disorders. Trends Neurosci 12:366–375. CrossRef Medline

Basso MA, Sommer MA (2011) Exploring the role of the substantia nigra pars reticulata in eye movements. Neuroscience 198:205–212. CrossRef Medline

Baufreton J, Kirkham E, Atherton JF, Menard A, Magill PJ, Bolam JP, Bevan MD (2009) Sparse but selective and potent synaptic transmission from the globus pallidus to the subthalamic nucleus. J Neurophysiol 102:532–545. CrossRef Medline

Bergman H, Wichmann T, Karmon B, DeLong MR (1994) The primate subthalamic nucleus. II. Neuronal activity in the MPTP model of parkinsonism. J Neurophysiol 72:507–520. Medline

Bernard V, Bolam JP (1998) Subcellular and subsynaptic distribution of the NR1 subunit of the NMDA receptor in the neostriatum and globus pallidus of the rat: co-localization at synapses with the GluR2/3 subunit of the AMPA receptor. Eur J Neurosci 10:3721–3736. CrossRef Medline

Bevan MD, Clarke NP, Bolam JP (1997) Synaptic integration of functionally diverse pallidal information in the entopeduncular nucleus and subthalamic nucleus in the rat. J Neurosci 17:308–324. Medline

Bevan MD, Magill PJ, Hallworth NE, Bolam JP, Wilson CJ (2002a) Regulation of the timing and pattern of action potential generation in rat subthalamic neurons in vitro by GABA-A IPSPs. J Neurophysiol 87:1348–1362. Medline

Bevan MD, Magill PJ, Terman D, Bolam JP, Wilson CJ (2002b) Move to the rhythm: oscillations in the subthalamic nucleus-external globus pallidus network. Trends Neurosci 25:525–531. CrossRef Medline

Bogacz R, Gurney K (2007) The basal ganglia and cortex implement optimal decision making between alternative actions. Neural Comput 19:442–477. CrossRef Medline

Bogacz R, Larsen T (2011) Integration of reinforcement learning and optimal decision-making theories of the basal ganglia. Neural Comput 23:817–851. CrossRef Medline

Boraud T, Bezard E, Guehl D, Bioulac B, Gross C (1998) Effects of L-DOPA on neuronal activity of the globus pallidus externalis (GPe) and globus pallidus internalis (GPi) in the MPTP-treated monkey. Brain Res 787:157–160. CrossRef Medline

Boraud T, Brown P, Goldberg J, Graybiel A, Magill P (2005) Oscillations in the basal ganglia: the good, the bad, and the unexpected. In: The basal ganglia VIII (Bolam JP, Ingham C, Magill P, eds), pp 1–24. New York: Springer.

Calabresi P, Picconi B, Tozzi A, Ghiglieri V, Di Filippo M (2014) Direct and indirect pathways of basal ganglia: a critical reappraisal. Nat Neurosci 17:1022–1030. CrossRef Medline

Cavanagh JF, Wiecki TV, Cohen MX, Figueroa CM, Samanta J, Sherman SJ, Frank MJ (2011) Subthalamic nucleus stimulation reverses mediofrontal influence over decision threshold. Nat Neurosci 14:1462–1467. CrossRef Medline

Collins AG, Frank MJ (2014) Opponent actor learning (OpAL): modeling interactive effects of striatal dopamine on reinforcement learning and choice incentive. Psychol Rev 121:337–366. CrossRef Medline

Cools R, Barker RA, Sahakian BJ, Robbins TW (2001) Mechanisms of cognitive set flexibility in Parkinson's disease. Brain 124:2503–2512. CrossRef Medline

Cragg SJ, Baufreton J, Xue Y, Bolam JP, Bevan MD (2004) Synaptic release of dopamine in the subthalamic nucleus. Eur J Neurosci 20:1788–1802. CrossRef Medline

Destexhe A, Sejnowski TJ (2003) Interactions between membrane conductances underlying thalamocortical slow-wave oscillations. Physiol Rev 83:1401–1453. Medline

Ding J, Peterson JD, Surmeier DJ (2008) Corticostriatal and thalamostriatal synapses have distinctive properties. J Neurosci 28:6483–6492. CrossRef Medline

Ding L, Gold JI (2010) Caudate encodes multiple computations for perceptual decisions. J Neurosci 30:15747–15759. CrossRef Medline

Ding L, Gold JI (2013) The basal ganglia's contributions to perceptual decision making. Neuron 79:640–649. CrossRef Medline

Fan KY, Baufreton J, Surmeier DJ, Chan CS, Bevan MD (2012) Proliferation

of external globus pallidus-subthalamic nucleus synapses following degeneration of midbrain dopamine neurons. J Neurosci 32:13718–13728. CrossRef Medline

Filion M, Tremblay L (1991) Abnormal spontaneous activity of globus pallidus neurons in monkeys with MPTP-induced parkinsonism. Brain Res 547:142–151. Medline

Forstmann BU, Dutilh G, Brown S, Neumann J, von Cramon DY, Ridderinkhof KR, Wagenmakers EJ (2008) Striatum and pre-SMA facilitate decision-making under time pressure. Proc Natl Acad Sci U S A 105: 17538–17542. CrossRef Medline

Frank MJ (2006) Hold your horses: a dynamic computational role for the subthalamic nucleus in decision making. Neural Netw 19:1120–1136. CrossRef Medline

Frank MJ, Samanta J, Moustafa AA, Sherman SJ (2007) Hold your horses: impulsivity, deep brain stimulation, and medication in parkinsonism. Science 318:1309–1312. CrossRef Medline

Frank MJ, Gagne C, Nyhus E, Masters S, Wiecki TV, Cavanagh JF, Badre D (2015) fMRI and EEG predictors of dynamic decision parameters during human reinforcement learning. J Neurosci 35:485–494. CrossRef Medline

Gatev P, Darbin O, Wichmann T (2006) Oscillations in the basal ganglia under normal conditions and in movement disorders. Mov Disord 21: 1566–1577. CrossRef Medline

Getting PA (1989) Emerging principles governing the operation of neural networks. Ann Rev Neurosci 12:185–204. CrossRef Medline

Gillies A, Willshaw D, Li Z (2002) Subthalamic-pallidal interactions are critical in determining normal and abnormal functioning of the basal ganglia. Proc Biol Sci 269:545–551. CrossRef Medline

Graham WC, Robertson RG, Sambrook MA, Crossman AR (1990) Injection of excitatory amino acid antagonists into the medial pallidal segment of a 1-methyl-4-phenyl-1,2,3,6-tetrahydropyridine (MPTP) treated primate reverses motor symptoms of parkinsonism. Life Sci 47:PL91–PL97. Medline

Graybiel AM (1995) Building action repertoires: memory and learning functions of the basal ganglia. Curr Opin Neurobiol 5:733–741. CrossRef Medline

Green N, Bogacz R, Huebl J, Beyer AK, Kühn AA, Heekeren HR (2013) Reduction of influence of task difficulty on perceptual decision making by STN deep brain stimulation. Curr Biol 23:1681–1684. CrossRef Medline

Gurney K, Prescott TJ, Redgrave P (2001a) A computational model of action selection in the basal ganglia. I. A new functional anatomy. Biol Cybern 84:401–410. CrossRef Medline

Gurney K, Prescott TJ, Redgrave P (2001b) A computational model of action selection in the basal ganglia. II. Analysis and simulation of behaviour. Biol Cybern 84:411–423. CrossRef Medline

Hammond C, Bergman H, Brown P (2007) Pathological synchronization in Parkinson's disease: networks, models and treatments. Trends Neurosci 30:357–364. CrossRef Medline

Hempel CM, Hartman KH, Wang XJ, Turrigiano GG, Nelson SB (2000) Multiple forms of short-term plasticity at excitatory synapses in rat medial prefrontal cortex. J Neurophysiol 83:3031–3041. Medline

Hikida T, Kimura K, Wada N, Funabiki K, Nakanishi S (2010) Distinct roles of synaptic transmission in direct and indirect striatal pathways to reward and aversive behavior. Neuron 66:896–907. CrossRef Medline

Hikosaka O (2007) Basal ganglia mechanisms of reward-oriented eye movement. Ann N Y Acad Sci 1104:229–249. CrossRef Medline

Hikosaka O, Isoda M (2010) Switching from automatic to controlled behavior: cortico-basal ganglia mechanisms. Trends Cogn Sci 14:154–161. CrossRef Medline

Hikosaka O, Wurtz RH (1983) Visual and oculomotor functions of monkey substantia nigra pars reticulata. I. Relation of visual and auditory responses to saccades. J Neurophysiol 49:1230–1253. Medline

Hikosaka O, Takikawa Y, Kawagoe R (2000) Role of the basal ganglia in the control of purposive saccadic eye movements. Physiol Rev 80:953–978. Medline

Holgado AJ, Terry JR, Bogacz R (2010) Conditions for the generation of beta oscillations in the subthalamic nucleus-globus pallidus network. J Neurosc 30:12340–12352. CrossRef Medline

Hsiao PY, Lo CC (2013) A plastic corticostriatal circuit model of adaptation in perceptual decision making. Front Comput Neurosci 7:178. CrossRef Medline

Hsieh MH, Gu SL, Ho SC, Pawlak CR, Lin CL, Ho YJ, Lai TJ, Wu FY (2012) Effects of MK-801 on recognition and neurodegeneration in an MPTP-induced Parkinson's rat model. Behav Brain Res 229:41–47. CrossRef Medline

Humphries MD, Stewart RD, Gurney KN (2006) A physiologically plausible model of action selection and oscillatory activity in the basal ganglia. J neurosci 26:12921–12942. CrossRef Medline

Kawagoe R, Takikawa Y, Hikosaka O (1998) Expectation of reward modulates cognitive signals in the basal ganglia. Nat Neurosci 1:411–416. CrossRef Medline

Kawagoe R, Takikawa Y, Hikosaka O (2004) Reward-predicting activity of dopamine and caudate neurons—a possible mechanism of motivational control of saccadic eye movement. J Neurophysiol 91:1013–1024. Medline

Kish LJ, Palmer MR, Gerhardt GA (1999) Multiple single-unit recordings in the striatum of freely moving animals: effects of apomorphine and D-amphetamine in normal and unilateral 6-hydroxydopamine-lesioned rats. Brain Res 833:58–70. CrossRef Medline

Kita H (2007) Globus pallidus external segment. Prog Brain Res 160:111–133. CrossRef Medline

Kita H, Kitai ST (1994) The morphology of globus-pallidus projection neurons in the rat—an intracellular staining study. Brain Res 636:308–319. CrossRef Medline

Kita H, Nambu A, Kaneda K, Tachibana Y, Takada M (2004) Role of ionotropic glutamatergic and GABAergic inputs on the firing activity of neurons in the external pallidum in awake monkeys. J Neurophysiol 92:3069–3084. CrossRef Medline

Kravitz AV, Tye LD, Kreitzer AC (2012) Distinct roles for direct and indirect pathway striatal neurons in reinforcement. Nat Neurosci 15:816–818. CrossRef Medline

Kumar A, Cardanobile S, Rotter S, Aertsen A (2011) The role of inhibition in generating and controlling Parkinson's disease oscillations in the basal ganglia. Front Syst Neurosci 5:86. CrossRef Medline

Leblois A, Boraud T, Meissner W, Bergman H, Hansel D (2006) Competition between feedback loops underlies normal and pathological dynamics in the basal ganglia. J Neurosci 26:3567–3583. CrossRef Medline

Lee JH, Whittington MA, Kopell NJ (2013) Top-down beta rhythms support selective attention via interlaminar interaction: a model. PLoS Comput Biol 9:e1003164. CrossRef Medline

Llinás RR (1988) The intrinsic electrophysiological properties of mammalian neurons: insights into central nervous system function. Science 242: 1654–1664. CrossRef Medline

Lo CC, Wang XJ (2006) Cortico-basal ganglia circuit mechanism for a decision threshold in reaction time tasks. Nat Neurosci 9:956–963. CrossRef Medline

Long MA, Fee MS (2008) Using temperature to analyse temporal dynamics in the songbird motor pathway. Nature 456:189–194. CrossRef Medline

Löschmann PA, De Groote C, Smith L, Wüllner U, Fischer G, Kemp JA, Jenner P, Klockgether T (2004) Antiparkinsonian activity of Ro 25-6981, a NR2B subunit specific NMDA receptor antagonist, in animal models of Parkinson's disease. Exp Neurol 187:86–93. CrossRef Medline

Lovinger DM, Tyler EC, Merritt A (1993) Short- and long-term synaptic depression in rat neostriatum. J Neurophysiol 70:1937–1949. Medline

Mallet N, Pogosyan A, Márton LF, Bolam JP, Brown P, Magill PJ (2008) Parkinsonian beta oscillations in the external globus pallidus and their relationship with subthalamic nucleus activity. J Neurosci 28:14245–14258. CrossRef Medline

Mallet N, Micklem BR, Henny P, Brown MT, Williams C, Bolam JP, Nakamura KC, Magill PJ (2012) Dichotomous organization of the external globus pallidus. Neuron 74:1075–1086. CrossRef Medline

McCarthy MM, Moore-Kochlacs C, Gu X, Boyden ES, Han X, Kopell N (2011) Striatal origin of the pathologic beta oscillations in Parkinson's disease. Proc Natl Acad Sci U S A 108:11620–11625. CrossRef Medline

Miguelez C, Morin S, Martinez A, Goillandeau M, Bezard E, Bioulac B, Baufreton J (2012) Altered pallido-pallidal synaptic transmission leads to aberrant firing of globus pallidus neurons in a rat model of Parkinson's disease. J Physiol 590:5861–5875. CrossRef Medline

Milenkova M, Mohammadi B, Kollewe K, Schrader C, Fellbrich A, Wittfoth M, Dengler R, Münte TF (2011) Intertemporal choice in Parkinson's disease. Mov Disord 26:2004–2010. CrossRef Medline

Mink JW (1996) The basal ganglia: focused selection and inhibition of competing motor programs. Prog Neurobiol 50:381–425. CrossRef Medline

Mitchell IJ, Carroll CB (1997) Reversal of parkinsonian symptoms in pri-

mates by antagonism of excitatory amino acid transmission: potential mechanisms of action. Neurosci Biobehav Rev 21:469–475. CrossRef Medline

Monchi O, Petrides M, Doyon J, Postuma RB, Worsley K, Dagher A (2004) Neural bases of set-shifting deficits in Parkinson's disease. J Neurosci 24:702–710. CrossRef Medline

Nevado-Holgado AJ, Mallet N, Magill PJ, Bogacz R (2014) Effective connectivity of the subthalamic nucleus-globus pallidus network during parkinsonian oscillations. J Physiol 592:1429–1455. CrossRef Medline

Newsome WT, Britten KH, Movshon JA (1989) Neuronal correlates of a perceptual decision. Nature 341:52–54. CrossRef Medline

Obeso JA, Rodríguez-Oroz MC, Rodríguez M, Lanciego JL, Artieda J, Gonzalo N, Olanow CW (2000) Pathophysiology of the basal ganglia in Parkinson's disease. Trends Neurosci 23:S8–S19. CrossRef Medline

Obeso JA, Marin C, Rodriguez-Oroz C, Blesa J, Benitez-Temino B, Mena-Segovia J, Rodriguez M, Olanow CW (2008) The basal ganglia in Parkinson's disease: current concepts and unexplained observations. Ann Neurol 64 [Suppl 2]:S30–S46. CrossRef Medline

Ogura M, Kita H (2000) Dynorphin exerts both postsynaptic and presynaptic effects in the globus pallidus of the rat. J Neurophysiol 83:3366–3376. Medline

Park C, Worth RM, Rubchinsky LL (2011) Neural dynamics in parkinsonian brain: the boundary between synchronized and nonsynchronized dynamics. Phys Rev E Stat Nonlin Soft Matter Phys 83:042901. CrossRef Medline

Pavlides A, Hogan SJ, Bogacz R (2012) Improved conditions for the generation of beta oscillations in the subthalamic nucleus–globus pallidus network. Eur J Neurosci 36:2229–2239. CrossRef Medline

Plenz D, Kital ST (1999) A basal ganglia pacemaker formed by the subthalamic nucleus and external globus pallidus. Nature 400:677–682. CrossRef Medline

Ratcliff R, Frank MJ (2012) Reinforcement-based decision making in corticostriatal circuits: mutual constraints by neurocomputational and diffusion models. Neural Comput 24:1186–1229. CrossRef Medline

Robert G, Drapier D, Verin M, Millet B, Azulay JP, Blin O (2009) Cognitive impulsivity in Parkinson's disease patients: assessment and pathophysiology. Mov Disord 24:2316–2327. CrossRef Medline

Roitman JD, Shadlen MN (2002) Response of neurons in the lateral intraparietal area during a combined visual discrimination reaction time task. J Neurosci 22:9475–9489. Medline

Roopun AK, Kramer MA, Carracedo LM, Kaiser M, Davies CH, Traub RD, Kopell NJ, Whittington MA (2008) Period concatenation underlies interactions between gamma and beta rhythms in neocortex. Front Cell Neurosci 2:1. CrossRef Medline

Rowe JB, Hughes L, Ghosh BC, Eckstein D, Williams-Gray CH, Fallon S, Barker RA, Owen AM (2008) Parkinson's disease and dopaminergic therapy—differential effects on movement, reward and cognition. Brain 131:2094–2105. CrossRef Medline

Rubin JE, McIntyre CC, Turner RS, Wichmann T (2012) Basal ganglia activity patterns in parkinsonism and computational modeling of their downstream effects. Eur J Neurosci 36:2213–2228. CrossRef Medline

Sadek AR, Magill PJ, Bolam JP (2007) A single-cell analysis of intrinsic connectivity in the rat globus pallidus. J Neurosci 27:6352–6362. CrossRef Medline

Sato F, Parent M, Levesque M, Parent A (2000) Axonal branching pattern of neurons of the subthalamic nucleus in primates. J Comp Neurol 424:142–152. CrossRef Medline

Sato M, Hikosaka O (2002) Role of primate substantia nigra pars reticulata in reward-oriented saccadic eye movement. J Neurosci 22:2363–2373. Medline

Selverston AI, Moulins M (1985) Oscillatory neural networks. Ann Rev Physiol 47:29–48. CrossRef Medline

Shen KZ, Johnson SW (2005) Dopamine depletion alters responses to glutamate and GABA in the rat subthalamic nucleus. Neuroreport 16:171–174. CrossRef Medline

Silberstein P, Pogosyan A, Kühn AA, Hotton G, Tisch S, Kupsch A, Dowsey-Limousin P, Hariz MI, Brown P (2005) Cortico-cortical coupling in Parkinson's disease and its modulation by therapy. Brain 128:1277–1291. CrossRef Medline

Smith GD, Cox CL, Sherman SM, Rinzel J (2000) Fourier analysis of sinusoidally driven thalamocortical relay neurons and a minimal integrate-and-fire-or-burst model. J Neurophysiol 83:588–610. Medline

Stanford IM, Cooper AJ (1999) Presynaptic μ and Δ opioid receptor modulation of GABAA IPSCs in the rat globus pallidus *in vitro*. J Neurosci 19:4796–4803. Medline

Steece-Collier K, Chambers LK, Jaw-Tsai SS, Menniti FS, Greenamyre JT (2000) Antiparkinsonian actions of CP-101,606, an antagonist of NR2B subunit-containing N-methyl-d-aspartate receptors. Exp Neurol 163:239–243. CrossRef Medline

Surmeier DJ, Shen W, Day M, Gertler T, Chan S, Tian X, Plotkin JL (2010) The role of dopamine in modulating the structure and function of striatal circuits. Prog Brain Res 183:149–167. CrossRef Medline

Tachibana Y, Iwamuro H, Kita H, Takada M, Nambu A (2011) Subthalamo-pallidal interactions underlying parkinsonian neuronal oscillations in the primate basal ganglia. Eur J Neurosci 34:1470–1484. CrossRef Medline

Tai LH, Lee AM, Benavidez N, Bonci A, Wilbrecht L (2012) Transient stimulation of distinct subpopulations of striatal neurons mimics changes in action value. Nat Neurosci 15:1281–1289. CrossRef Medline

Terman D, Rubin JE, Yew AC, Wilson CJ (2002) Activity patterns in a model for the subthalamopallidal network of the basal ganglia. J Neurosci 22:2963–2976. Medline

Wang XJ (2002) Probabilistic decision making by slow reverberation in cortical circuits. Neuron 36:955–968. CrossRef Medline

Wichmann T, Soares J (2006) Neuronal firing before and after burst discharges in the monkey basal ganglia is predictably patterned in the normal state and altered in parkinsonism. J Neurophysiol 95:2120–2133. Medline

Wiecki TV, Frank MJ (2013) A computational model of inhibitory control in frontal cortex and basal ganglia. Psychol Rev 120:329–355. CrossRef Medline

Wilson CJ (2013) Active decorrelation in the basal ganglia. Neuroscience 250:467–482. CrossRef Medline

Zavala B, Brittain JS, Jenkinson N, Ashkan K, Foltynie T, Limousin P, Zrinzo L, Green AL, Aziz T, Zaghloul K, Brown P (2013) Subthalamic nucleus local field potential activity during the Eriksen flanker task reveals a novel role for theta phase during conflict monitoring. J Neurosci 33:14758–14766. CrossRef Medline

Zavala BA, Tan H, Little S, Ashkan K, Hariz M, Foltynie T, Zrinzo L, Zaghloul KA, Brown P (2014) Midline frontal cortex low-frequency activity drives subthalamic nucleus oscillations during conflict. J Neurosci 34:7322–7333. CrossRef Medline